Environmental Science & Technology

Article

pubs.acs.org/est

Photoreactivity of Unfunctionalized Single-Wall Carbon Nanotubes Involving Hydroxyl Radical: Chiral Dependency and Surface Coating Effect

Wen-Che Hou,*[,†,‡] Somayeh BeigzadehMilani,[§] Chad T. Jafvert,[§] and Richard G. Zepp*[,∥]

[†]National Exposure Research Laboratory, Ecosystems Research Division, U.S. Environmental Protection Agency, Athens, Georgia 30605, United States

[‡]Department of Environmental Engineering, National Cheng Kung University, Tainan City 70101, Taiwan

[§]Division of Environmental and Ecological Engineering and School of Civil Engineering, Purdue University, West Lafayette, Indiana 47907, United States

[∥]National Exposure Research Laboratory, Ecosystems Research Division, U.S. Environmental Protection Agency, Athens, Georgia 30605, United States

Supporting Information

ABSTRACT: Single-wall carbon nanotubes (SWCNTs) have a variety of potential and demonstrated applications, and their production rates are increasing rapidly. This increase in production has motivated research on their transport and potential transformation and their toxicity in the environment. In this work, we examined the direct and indirect photoreactivity of SWCNTs under sunlight conditions. We found that the direct photoreactivity of pristine SWCNTs is generally low; however, indirect photoreaction involving ·OH may be significant in natural aquatic environments. Environmental photochemical reactions generating ·OH lead to distinct changes in SWCNT fluorescence efficiency in the near-infrared (NIR) region, Raman spectra, and light attenuation spectra in the UV, visible, and NIR regions, indicating that covalent functionalization of SWCNTs occurs. The reactivity of SWCNTs to ·OH is dependent on the specific chiral structure of the SWCNTs and the surfactant associated with it. An operationally defined second-order rate constant (based on the decrease in NIR fluorescence signals) for all SWCNT chiral species reacting with ·OH was estimated to be $(2.91 \pm 1.30) \times 10^{10}$ M^{-1} s^{-1}. Our work suggests that photochemical reactions may be a significant transformation pathway of SWCNTs in aquatic systems.

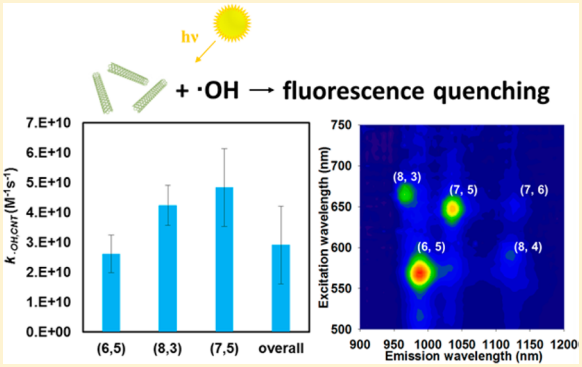

INTRODUCTION

Single-wall carbon nanotubes (SWCNTs) are an important class of fullerenes that can be structurally conceptualized as a one-atom-thick layer of graphene wrapped into a seamless cylinder of sp^2-hybridized carbon atoms and arranged in repeating hexagonal aromatic rings. SWCNTs and their derivatives are emerging in a range of industrial applications and consumer products, especially in high-performance microelectronics as transistors (e.g., thin-film transistor displays) and biosensors.[1] For applications in electronic and optoelectronic devices and photovoltaics, pristine, unfunctionalized SWCNTs are desired due to their unique electronic properties (e.g., metallic and semiconducting characters, high carrier mobility, etc.) that are compromised upon covalent sidewall functionalization that destroys the sp^2-hybridized carbon structure.[2,3] SWCNTs may be released from these products during their life cycles and enter ecosystems where they can be chemically or biologically transformed and degraded by photolytic, abiotic chemical, and enzymatic reactions.[4,5]

There is limited research reporting how carbon nanotubes react in the environment. Allen et al. demonstrated that carboxylated SWCNTs could react enzymatically in the presence of H_2O_2 and horseradish peroxidase (HRP), a plant-derived enzyme, resulting in significant degradation of the SWCNT structure, with some mineralization to CO_2.[6] Interestingly, unfunctionalized (i.e., pristine) SWCNTs are largely nonreactive in HRP-mediated systems, indicating that surface functionalization plays a role in their overall reactivity, as expected. It was suggested that the hydrophobicity of unfunctionalized SWCNTs prevents interaction with the HRP reactive site, which is an Fe(IV) porphyrin radical cation.[7] However, when a Fenton-like reaction involving $FeCl_3$ and H_2O_2 was applied, both carboxylated and pristine SWCNT

Received: January 2, 2014
Revised: March 12, 2014
Accepted: March 14, 2014
Published: March 14, 2014

 © 2014 American Chemical Society dx.doi.org/10.1021/es500013j | Environ. Sci. Technol. 2014, 48, 3875−3882

were degraded, indicating that homolytic cleavage of H_2O_2 produces free radicals (likely hydroxyl radicals (·OH)) that react with SWCNT.[7]

Current manufacturing processes generally produce heterogeneous SWCNT materials with mixed chiralities, and hence mixed electronic (metallic or semiconducting) properties.[8] These characteristics can be seen in UV−visible-near-infrared (NIR) absorbance spectra due to the strong chirality-dependent photoelectronic transitions.[9] This light absorption also suggests that SWCNTs may be photoreactive. Indeed, Grandra et al. showed that pristine SWCNTs suspended in water could photosensitize $^1O_2$ formation upon exposure to 532 nm laser light, via a two-photon absorption process.[10] Chen et al. and Chae et al. reported that functionalized SWCNTs could generate a range of reactive oxygen species (ROS), including $^1O_2$ and ·OH under UVA light or sunlight exposure, whereas pristine SWCNTs dispersed in surfactant solution was fairly inert.[11−13] Additional work by Petersen et al. indicates that SWCNTs could scavenge or react with ROS including ·OH in simulated biological systems involving SWCNT and DNA under ultrasonication.[14] Light exposure also can induce the transformation of some SWCNTs. For example, Alvarez et al. demonstrated that pristine SWCNTs could be photohydroxylated in the absence of dissolved O_2 under UV 254 nm light irradiation.[15] This suggests that reactive intermediates, such as ·OH generated during photolysis, could be responsible for SWCNT transformation.[15] In this particular study, no H_2O_2 (a precursor of ·OH under light exposure) was added. Another study that reported on irradiating SWCNTs in 30% H_2O_2 under visible light (400−700 nm) indicated that SWCNTs significantly react, as indicated by the loss of the SWCNT's intrinsic NIR fluorescence, and that reaction with ·OH may have been the cause.[16,17] However, quantification of ·OH was not performed in parallel with the observed decrease in SWCNT fluorescence, making it difficult to predict the rate that may occur in natural aquatic systems.

Upon entering the aquatic environment, SWCNTs can associate with naturally occurring and anthropogenic macromolecules such as natural organic matter (NOM) and surfactants, affecting their fate and transport. For example, NOM significantly enhances the dispersion of otherwise strongly aggregated pristine carbon nanotubes in Suwannee River water samples or simulated natural waters containing NOM,[18,19] indicating the possibility of NOM facilitating aquatic transport of carbon nanotubes. Interaction with man-made macromolecules may also occur. Research on the environmental transport of unfunctionalized SWCNTs associated with anthropogenic surfactant macromolecules is increasing.[20−22] For example, Bouchard et al. reported that pristine SWCNTs could be stabilized for months in river water samples in the presence of sodium dodecyl sulfate (SDS) at 0.001% (w/v), a concentration that can be found in wastewater effluents.[20] Interaction with these materials will affect their reactivity. For example, NOM is a well-known photosensitizer, producing a range of reactive transients such as ·OH that may react with SWCNTs.[23,24] The photo-Fenton reaction and nitrate photolysis are additional sources of ·OH in sunlit natural waters.[25,26]

In this study, we provide new data on unfunctionalized SWCNT direct photoreactions and indirect photochemical reactions involving ·OH, generated from H_2O_2 under solar wavelength exposures. We selected two SWCNT materials produced by two typical but distinct synthesis processes that lead to products with different diameters, chiralities, and electronic properties. Because of the strong bundling of pristine SWCNTs in water, SWCNT materials were dispersed in aqueous solutions containing SDS or sodium deoxycholate (SDOC). The addition of the surfactants resulted in well-dispersed unbundled carbon nanotubes, enabling the use of UV−visible-NIR absorbance and NIR fluorescence for tracking the photoreactions as a function of chirality. We show that the pristine SWCNTs we studied are fairly nonreactive under direct sunlight exposure, yet they react when ·OH is present. Larger diameter SWCNTs react more rapidly with ·OH than the smaller diameter SWCNTs, and the reaction rate with ·OH is dependent on the type of surfactant present, with SDOC-associated SWCNT being less reactive. This work suggests that SWCNT can undergo indirect photochemical transformation through reaction with ·OH, with reaction rate dependent on chirality.

■ MATERIALS AND METHODS

Materials. Two SWCNT materials were used in this study and were obtained from the National Institute of Standards and Technology (NIST) (SRM 2483) and NanoIntegris, Inc. (Menlo Park, CA). NIST originally obtained the SWCNT material from SouthWest NanoTechnologies, Inc. (Norman, OK) and standardized it as SRM 2483. According to SouthWest NanoTechnologies, Inc., the sample is made by using the CO disproportionation method catalyzed by cobalt and molybdenum (i.e., the CoMoCAT process).[27] The sample was predominately semiconducting tubes (>95%) that are enriched in the (6, 5) chiral species (>40%). The sample hereafter is referred to as SG65 SWCNT. The SWCNT sample from NanoIntegris was synthesized by the high-pressure CO conversion process (HiPco) and contained both semiconducting and metallic tubes.[28−30] According to the supplier, the HiPco SWCNT sample had a carbon content >95%, and tube diameters ranged from 0.8 to 1.2 nm. Other chemicals were of the highest purity available from Sigma Aldrich (St. Louis, MO) and used without further purification. All aqueous samples were prepared using water purified with an Aqua Solutions 2121BL system (≥18.0 MΩ).

Aqueous Dispersions of SWCNT. SWCNT material (10 mg) was added to 40 mL of 1% (w/w) aqueous SDS or SDOC. The mixture was probe-sonicated (XL2020; 550 W; 20 kHz; Misonix, Inc.; Farmingdale, NY) in an ice−water bath to minimize potential SWCNT oxidation arising from the heat generated during sonication. The energy amplitude of the sonicator was adjusted to 30%, and the duration was set for the time at which the sample received about 2 000 J/mL of energy. The resulting samples were centrifuged (model 5424, Eppendorf) at 21 000 g for 2 h, and 80% of the supernatant was collected for use. The SWCNT concentration was standardized using the UV−visible-NIR absorption spectra according to the Beer−Lambert law.[31] The procedure and discussion regarding the UV−visible-NIR absorbance measurement are presented in the Supporting Information. Some SWCNT samples were spiked with concentrated 30% H_2O_2 to achieve a 100 mM H_2O_2 concentration prior to irradiation. The samples were not pH-buffered, and the initial pH was measured to be about 7.0.

Irradiation. Experiments were performed in an Atlas SunTest CPS+ solar simulator (Atlas Materials Testing Technology, Chicago, IL), equipped with a 1 kW xenon arc lamp. The reaction vessels were 8 mL Pyrex tubes to which 5

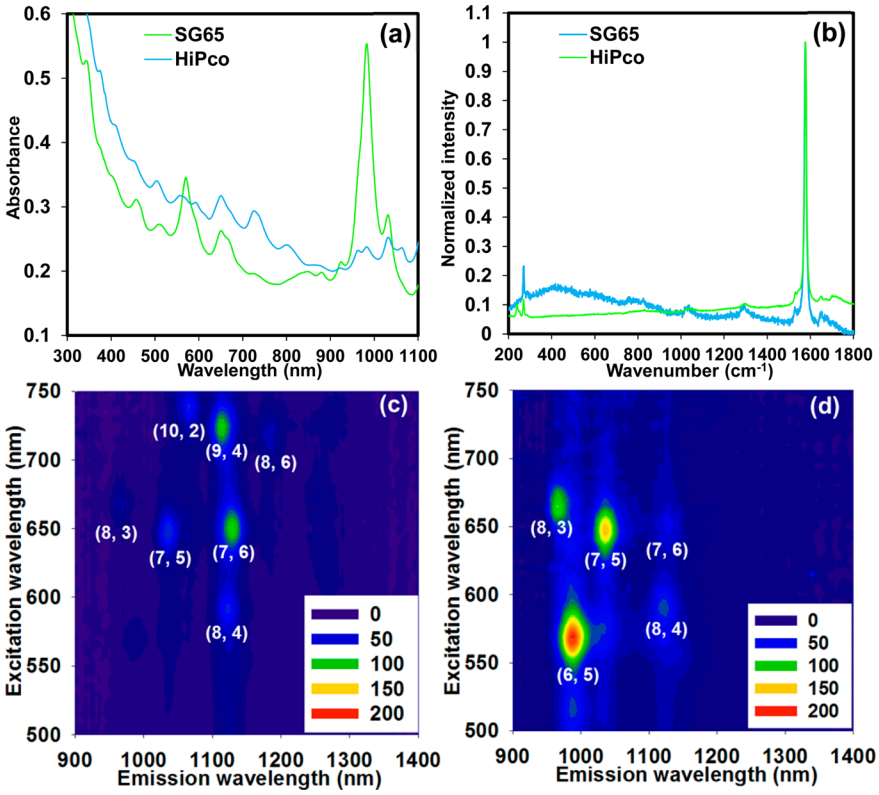

Figure 1. Characterization of single-wall carbon nanotube (~8.0 mg/L) dispersed in 1% SDOC aqueous solutions, indicating (a) the UV−visible-NIR absorbance, (b) the Raman spectra, and the excitation−emission matrix (EEM) of (c) HiPco sample and (d) SG65 sample.

mL of reaction solution was added. During irradiation, the tubes were completely submersed in a thermostatted water bath (25 °C). The spectrum of the solar simulator light can be found in our earlier publication.[32] The incident light intensity at the tube surface, summed from 290 to 700 nm, was 0.065 W/cm^2. For kinetic studies, we prepared a series of tubes for irradiation. At specific times during irradiation, one tube was removed from the reactor and sacrificed for material analysis. Dark control tubes were wrapped with aluminum foil and irradiated concurrently. All experiments were performed in duplicate or triplicate.

To examine the effect of O_2, dissolved O_2 was removed from SWCNT aqueous dispersions in a N_2 glovebox. The samples were kept in the glovebox for 2 days prior to further use. The N_2 glovebox actively removed trace O_2 by a Pd-catalyzed reaction, and O_2 concentration was undetectable by an O_2 sensor (model 10, Coy Laboratory Products, Inc., Grass Lake, MI). The accuracy of the O_2 sensor is in the range of 20−700 ppm. Sample tubes containing the deoxygenated sample were sealed with PTFE-lined caps in the glovebox prior to removal for irradiation.

Analysis. The SWCNT photoreactions were followed using a Perkin-Elmer Lambda 35 UV−visible-NIR absorption spectrophotometer with a 1 cm quartz cuvette. A Horiba Fluorolog 3-221 spectrofluorometer was used to monitor the change in semiconducting SWCNT's band gap fluorescence [or photoluminescence (PL)] after light exposure. The spectrofluorometer was equipped with an InGaAs near-IR detector cooled by liquid N_2. The spectra were corrected for variations in wavelength-dependent excitation intensity and detector sensitivity. Prior to fluorometry, sample pH was adjusted to 8.0 to ensure that any loss of PL was not due to protonation-induced quenching that is characteristic of SWCNTs.[33] The SWCNT photoproducts were also characterized by using a Renishaw inVia Raman spectrophotometer. A 633 nm laser beam was used to excite the liquid SWCNT samples in the Raman spectrophotometer. The steady-state ·OH concentration in the system was quantitated using 1.5 μM *para*-chlorobenzoic acid (*p*CBA) as a chemical probe. *p*CBA was added to SWCNT dispersions and irradiated identically to experimental SWCNT samples that did not contain *p*CBA. *p*CBA was quantified by HPLC using a UV detector. The SWCNTs were removed by passage of the dispersions through 0.22 μm membrane filters prior to HPLC analysis. To account for the potential sorption of *p*CBA to SWCNT, we prepared control samples that were not exposed to light. The loss of *p*CBA due to its reaction with ·OH was measured by the difference in *p*CBA concentration between control and experimental samples.

RESULTS AND DISCUSSION

Characterization of SWCNT Dispersions. SWCNT samples were characterized using UV−visible-NIR absorbance, near-infrared fluorescence (NIRF), and Raman spectroscopy to deduce their state of dispersion, initial chirality, changes in their electronic properties, and degree of surface functionalization. The sharp optical absorbance peaks characteristic of the interband transitions of well-dispersed SWCNTs are shown in Figure 1a. For example, the absorbance intensity ratio of the (6, 5) chiral nanotube of the SG65 sample at ~984 nm, to the baseline absorbance at 905 nm (i.e., not belonging to transition of any SWCNT species), is 2.60, which is comparable to values reported in the literature for debundled SWCNT samples.[31] It

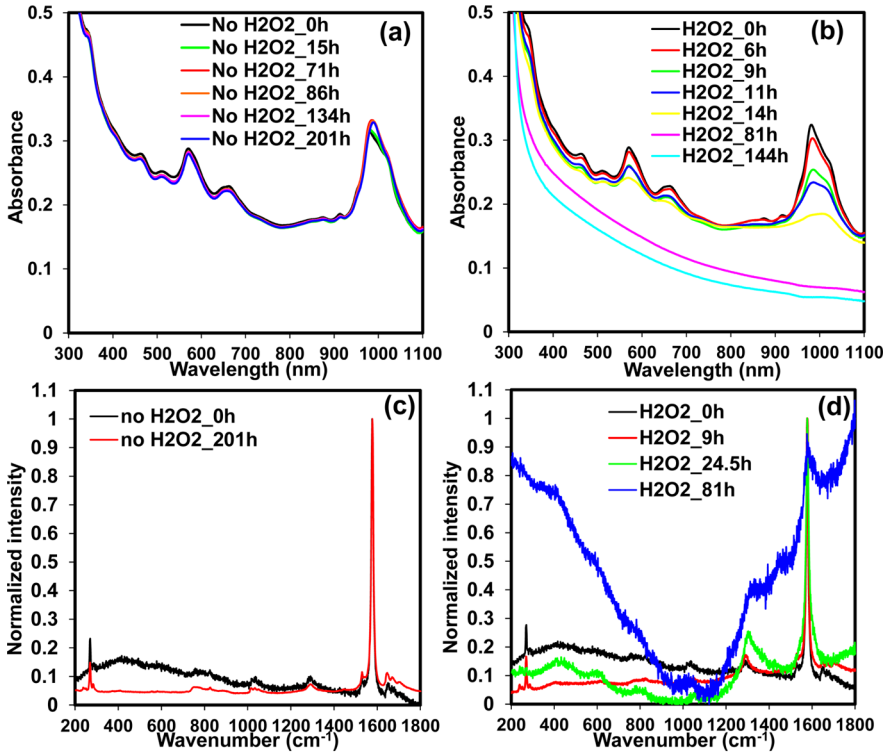

Figure 2. Phototransformation of SG65 SWCNT as indicated by UV−visible-NIR absorbance in samples containing (a) no H_2O_2 and (b) 100 mM H_2O_2 and by Raman spectroscopy of samples containing (c) no H_2O_2 and (d) 100 mM H_2O_2. SG65 SWCNT sample was dispersed in 1% SDS. The spectra are the averages of at least two replicate samples.

has been reported that this fine spectral structure could be obscured by intertube coupling of bundled SWCNT.[34]

The Raman spectra of the SG65 and HiPco SWCNT samples (Figure 1b) reveal the radial breathing mode (RBM) at 200−300 cm^{-1} and tangential mode at 1579 cm^{-1} (i.e., the G band) characteristic of sp^2 carbon.[35] The disorder mode (D band) at 1295 cm^{-1}, diagnostic of covalent functionalization of SWCNT side walls, is rather small, indicating these SWCNT samples were not significantly oxidized during dispersion by sonication.[35]

NIRF spectra of SG65 and HiPco SWCNT samples in EEM are reported in Figure 1c,d. NIRF spectroscopy has been used to detect SWCNTs in the environment, and the spectral features of NIR emission corresponding to the band gap energy of specific semiconducting SWCNT chiralities have been used to determine structural information.[29,36−38] The HiPco SWCNT sample contained mostly (8, 3), (7, 5), (8, 4), (7, 6), (10, 2), (9, 4), and (8, 6) chiral nanotubes (Figure 1c), whereas the SG65 sample was dominated by (6, 5) chiral nanotube with (8, 3), (7, 5), (8, 4), and (7, 6) species also present (Figure 1d). The strong photoluminescence (PL) of these samples is another indication that the SWCNTs are exfoliated from bundles and contain few surface defects (i.e., destruction of sp^2 hybridization), as SWCNT PL would be quenched by bundling and/or covalent functionalization.[29,39,40] The SWCNT dispersed in SDS (data not shown) exhibits characteristics similar to those presented in Figure 1a-d.

Photoreaction of SWCNTs in Solar Spectrum Light. Upon exposure to the lamp light, the UV−visible-NIR absorbance of SG65 SWCNTs decreased in the presence of H_2O_2 (Figure 2b) but not in suspensions of SWCNTs alone (Figure 2a). Reaction with ·OH, generated by H_2O_2 photolysis, likely occurs, leading to surface-disordered SWCNTs as a result of oxidative functionalization, leading to surface-disordered SWCNTs. This is consistent with the Raman spectra where the increase in the D to G band ratio from 0.1 to 0.45 after 81 h of exposure indicates the destruction of sp^2 carbon bonds (Figure 2d). In contrast, the Raman spectra for SG65 SWCNT samples in the absence of H_2O_2 remained the same after exposure (Figure 2c). Similar results (i.e., H_2O_2-dependence) were observed for HiPco SWCNT samples (Supporting Information Figure S1).

NIRF spectra of the same samples are presented in Figure 3. The spectral evolution in PL was not uniform, indicating that differences in reactivity as a function of chirality occurred and may lead to important changes of SWCNT mixtures upon weathering in the environment. For example, the PL loss of the (6, 5) tubes was less rapid than that of the (8, 3) and (7, 5) tubes, indicating lower susceptibility of the (6, 5) tubes to ·OH attack, at least with respect to residual PL. Nevertheless, the PL for all chiral components disappeared completely after 14 h of light exposure. Interestingly, a strong increase in the PL occurred at the region centered at an excitation of 570 nm and emission of 1120 nm, which can be attributed to the midgap emission of (6, 5) chiral tube products. The midgap emission of (6, 5) chiral tubes has been reported previously. McDonald et al. showed that SWCNTs react with highly concentrated 15% (w/v) H_2O_2 in the dark resulting in an EEM similar to what we report in Figure 3b,c.[41] Although the specific oxidant that reacted with the SWCNTs was unknown in this earlier study, it was suggested that ·OH, generated from H_2O_2 and residual metal catalysts inherent in SWCNT samples (i.e., Fenton-like reaction), was responsible.[41] We observed no changes in PL of the SWCNT samples in the dark within our experimental time

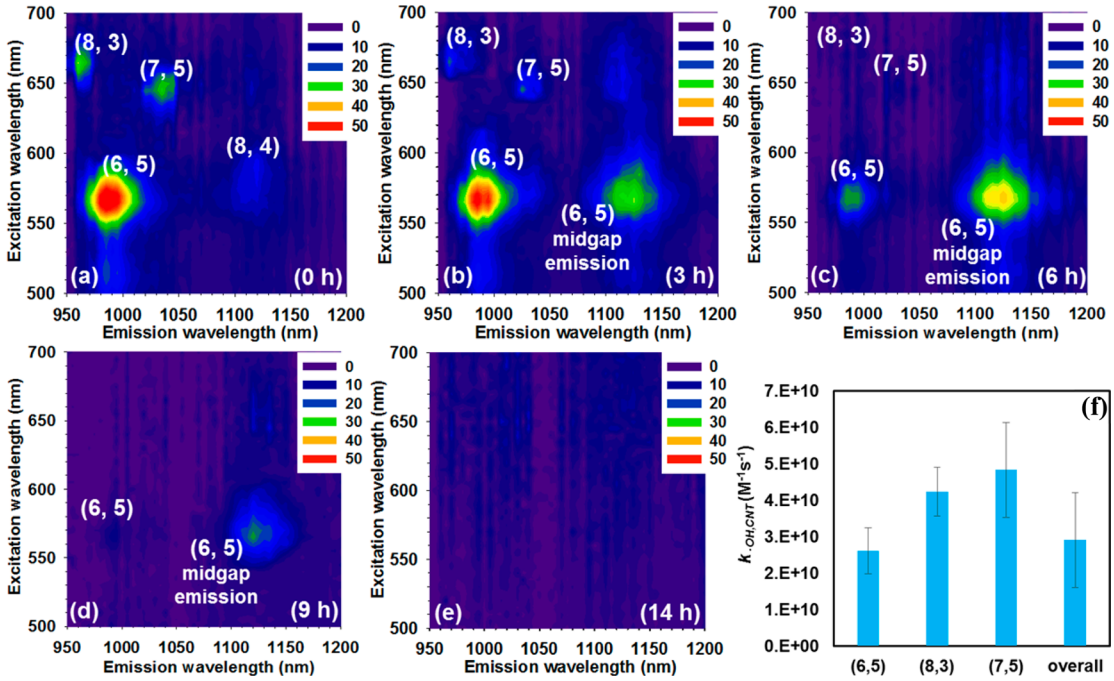

Figure 3. Time-resolved EEM showing (a−e) the fluorescence quenching of SG65 SWCNT in the presence of 100 mM H_2O_2 under sunlight exposure at pH = 7.0. Panel f indicates the operationally defined second-order rate constants for ·OH reaction with different chiral components and with SWCNTs as a whole. The SG65 SWCNT sample was dispersed in 1% SDS. The error bars indicate 95% confidence intervals.

scale, possibly due to the much lower H_2O_2 concentrations we used. A similar observation is also reported in a recent study by Piao et al. who showed a red-shifted PL of (6, 5) SWCNT upon reacting with diazonium salts.[42] Density functional theory calculations suggest that the reaction creates defects that split the doubly degenerate frontier orbitals of a SWCNT, creating an optically allowed, low-lying state from which the new PL derives.[42] A related study by Alvarez et al. using N_2-saturated SWCNT samples without H_2O_2 present and irradiation with 254 nm light showed that the PL of SWCNTs with smaller diameters was quenched more rapidly.[15] This result is different from ours and that of McDonald et al., suggesting that reactivity under the different conditions may involve different mechanisms and reactive species. Our results are consistent with earlier reports showing that oxidative processes involving organic electron acceptors occur most rapidly with large-diameter SWCNTs that have small band gaps.[40] An alternative explanation for the chirality-dependent reactivity is that, analogous to selective reactions of amino acid moieties within proteins with ·OH[43] or singlet oxygen,[44] the reactive sites on the (6, 5) tube surfaces are partially blocked from reaction with ·OH, a steric effect that could result from the stronger physical binding interaction of charged dodecylsulfate (DS^-) with a smaller diameter SWCNT [i.e., the (6, 5) tube] that acts to stabilize the (6, 5) tubes within the dispersion.[41]

In further experiments, octanol, an ·OH scavenger ($k_{\cdot OH,OCT} = 6 \times 10^9\ M^{-1}\ s^{-1}$), was added to test the intermediacy of ·OH (Supporting Informaion Figure S2). The reduction in the steady-state ·OH concentration quantitatively correlates with the decrease in the quenching rates of the SWCNT's band gap fluorescence (Supporting Information Figure S2), indicating the intermediacy of ·OH in SWCNT transformation. The detailed kinetic analysis of ·OH reaction involving DS^- and octanol quenchers is presented in the Supporting Information. We measured the steady-state ·OH concentration in SG65 SWCNT suspensions in 1% SDS to be $(2.44 \pm 0.44) \times 10^{-15}$ M (error indicates 95% confidence interval (CI)). Assuming that the pristine SWCNT "relative" concentration can be approximated by the PL intensity volume, calculated by integrating the areas under all the EEM region, indicative of all SWCNT semiconducting components as shown in Figure 3,[36,37] the pseudo-first-order rate constant for SWCNT reaction (in terms of fluorescence-quenching) is estimated to be $(7.1 \pm 1.4) \times 10^{-5}\ s^{-1}$ (error indicates 95% CI). The kinetic traces are presented in Figure S3 in theSupporting Information. Assuming that the reaction is first-order in ·OH, the second-order rate constant for SWCNT reacting with ·OH is obtained by dividing this pseudo-first-order rate constant by the steady-state ·OH concentration (i.e., using equation S5 in theSupporting Information). The calculated second-order rate constant for all chiral components combined is $(2.91 \pm 1.30) \times 10^{10}\ M^{-1}\ s^{-1}$ (error indicates 95% CI). Because reaction is followed by PL loss, the units of molarity on the rate constant result from the steady-state concentration of ·OH in the "apparent" second-order reaction. We note that this operationally defined second-order rate constant should not be directly compared to those of ·OH reacting with molecular compounds because the dependence of "degree of functionalization" with PL loss is unknown, and the dynamics of diffusion in water between homogeneous solutions and heterogeneous dispersions is an important complicating factor. Nevertheless, the loss of PL indicates that the covalent surface functionalization of SWCNT as a result of the reaction with ·OH leads to the conversion of sp^2-hybridized carbon atoms to sp^3 hybridization that disrupts semiconducting SWCNT's electronic band gap structure from which the PL derives. This process obeys pseudo-first-order kinetics (Supporting Information Figure S3) as expected, assuming that the ·OH concentrations are steady-state and that the amount of sp^2-hybridized carbon atoms on the surfaces of SWCNT is the only variable. The respective second-order rate

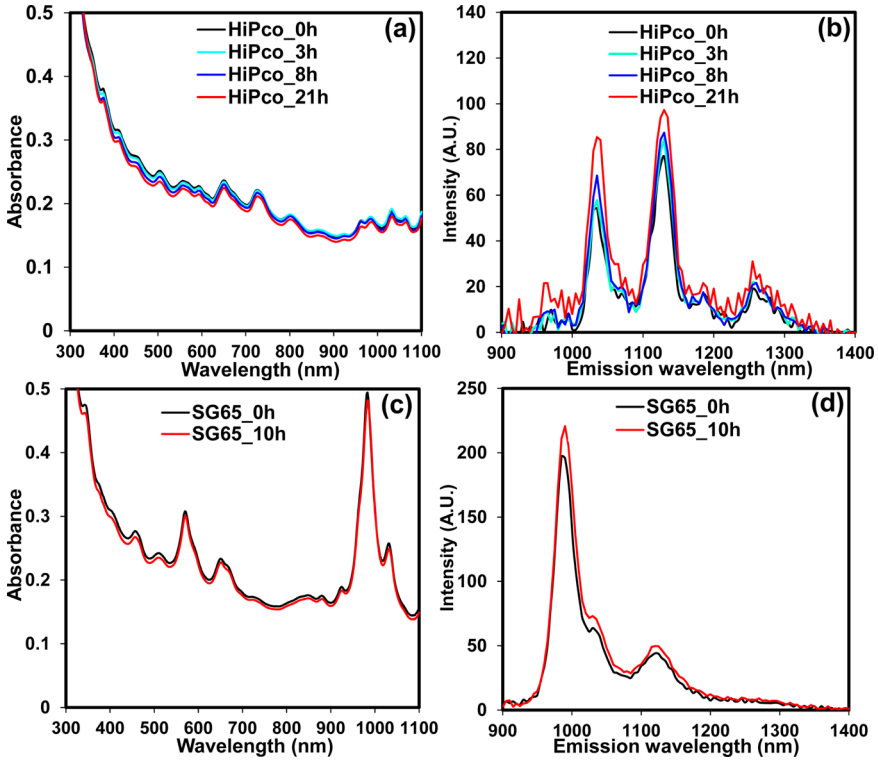

Figure 4. Phototransformation of SWCNT dispersed in 1% SDOC in the presence of 100 mM H_2O_2 under sunlight exposure at pH = 7.0. (a and c) UV−visible-NIR absorbance and (b and d) NIRF spectra for (a and b) HiPco and (c and d) SG65 samples. The excitation wavelengths used were 567 and 640 nm for SG65 SWCNT and HiPco SWCNT samples, respectively, in the NIRF analyses. The spectra are the averages of at least two replicate samples.

constants of the chiral components are presented in Figure 3f. The reaction rate for the (8, 4) chiral species is not presented because its PL partially overlaps with the (6, 5) midgap emission.

Effect of SWCNT Surface Coating. Reactivity of SWCNT samples dispersed in 1% SDOC with ·OH is presented in Figure 4. Both SG65 and HiPco SWCNT samples were less reactive in deoxycholate (DOC^-) even though the measured steady-state ·OH concentration in the DOC^- system was about three times greater, suggesting that DOC^- could shield SWCNT against ·OH attack (Figure 4). DOC^- possesses a rigid planar structure that may allow it to form a tightly packed monolayer on the SWCNT surfaces, in contrast to the more flexible linear chains of DS^- which loosely pack on SWCNT surfaces.[45−48] The surfactant structural packing may play a role in the reactivity of SWCNT-surfactant assemblies. For example, Hilmer et al. demonstrated that organic oxidants react with SWCNTs that are coated with DS^- much more rapidly than with SWCNTs covered with DOC^-, which is consistent with our observations using ·OH as the oxidant.[49] It was suggested that tight packing of DOC^- on SWCNT surfaces could impart a steric effect, decreasing the rate of reactants contacting the SWCNT surface.

Another possibility is that, although ·OH clearly initiates the loss of fluorophores within the SWCNTs, there may be some involvement by DS^- above and beyond its dispersive properties and ·OH scavenging abilities. This may involve, for example, reactions of ·OH with DS^- producing intermediate free radicals that ultimately are involved in reactions with the SWCNTs.

In additional experiments, we tested water quality parameters including the dissolved O_2 concentration, the presence of Suwannee River humic acid (SRHA), and addition of a real river water sample (Oconee River, Athens, GA) on the photoreactivity of SWCNTs in 1% SDS. Because these conditions did not change the SWCNT's photoreactivity, they are reported in the Supporting Information (Text S3 and Figures S4−S6).

Environmental Significance. Upon release into aquatic systems, pristine SWCNTs could interact with natural or anthropogenic organic macromolecules and become dispersed in water. Alternatively, SWCNTs dispersed in surfactants could enter the water columns where they could be stable for some time before significant surfactant dilution occurs or the local water chemistry supports dispersion (e.g., high NOM concentration). Our work indicates that dispersed unfunctionalized SWCNTs are fairly inert under direct sunlight exposure but react with ·OH that is very often photochemically generated in natural waters, indicating that reaction with ·OH may be a transformation process of SWCNTs in the environment. Considering that $[OH]_{ss}$ near the surface of many freshwaters is generally in the range of 10^{-15} to 10^{-17} M during daylight at a latitude of 40° N in the summer, the estimated near-surface pseudo-first-order rate constants for photochemical transformation (as measured by PL loss) for the SWCNTs investigated in this study range from 0.01 to 0.1 h^{-1}. Corresponding half-lives for PL loss are estimated to be in the range of 7−660 h. The reactivity, as measured by PL loss, with ·OH is dependent on the chirality and type of associated surfactant. Findings such as these may eventually inform manufacturing methods of and product applications for SWCNTs and other carbonaceous nanomaterials that reduce environmental impact through production and use of SWCNTs that are more susceptible to environmental degradation, where applicable.

■ ASSOCIATED CONTENT

Supporting Information

Additional information on the procedure for UV−visible-NIR absorbance measurement, photoreactivity of HiPco SWCNTs, hydroxyl radical effects on SWCNT fluorescence quenching, a detailed kinetic analysis, kinetic trace of PL quenching, influence of water quality parameters including dissolved O_2 concentration, the presence of SRHA, and use of a real river water sample on the photoreactivity of SWCNT. This material is available free of charge via the Internet at http://pubs.acs.org.

■ AUTHOR INFORMATION

Corresponding Author

*Phone: +886 6 2757575 ext. 65842 (W.C.H.); (706) 355-8117 (R.G.Z.). E-mail: whou@mail.ncku.edu.tw (W.C.H.); zepp.richard@epa.gov (R.G.Z.).

Notes

The authors declare no competing financial interest.

■ ACKNOWLEDGMENTS

This article has been reviewed in accordance with the U.S. Environmental Protection Agency's (U.S. EPA) peer and administrative review policies and approved for publication. Mention of trade names or commercial products does not constitute an endorsement or recommendation for use by the U.S. EPA. Financial support provided by the National Science Council (NSC) of Taiwan (for W.-C. Hou) under Grant Number NSC 102-2218-E-006-016 is acknowledged. This research was, in part, supported by the Ministry of Education, Taiwan, R.O.C., The Aim for the Top University Project to the National Cheng Kung University (NCKU). Financial support (for C. T. Jafvert and S. BeigzadehMilani) provided by the EPA STAR program, Grant 83485801, is also acknowledged.

■ REFERENCES

(1) Volder, M. F. L. D.; Tawfick, S. H.; Baughman, R. H.; Hart, A. J. Carbon nanotubes: Present and future commercial applications. *Science* **2013**, *339*, 535−539.

(2) Zhao, Y.-L.; Stoddart, J. F. Noncovalent functionalization of single-walled carbon nanotubes. *Acc. Chem. Res.* **2009**, *42*, 1161−1171.

(3) Clavé, G.; Delport, G.; Roquelet, C.; Lauret, J.-S.; Deleporte, E.; Vialla, F.; Langlois, B.; Parret, R.; Voisin, C.; Roussignol, P.; et al. Functionalization of carbon nanotubes through polymerization in micelles: A bridge between the covalent and noncovalent methods. *Chem. Mater.* **2013**, *25*, 2700−2707.

(4) Nowack, B.; Ranville, J. F.; Diamond, S.; Gallego Urrea, J. A.; Metcalfe, C.; Rose, J.; Horne, N.; Koelmans, A. A.; Klaine, S. J. Potential scenarios for nanomaterial release and subsequent alteration in the environment. *Environ. Toxicol. Chem.* **2012**, *31*, 50−59.

(5) Petersen, E. J.; Zhang, L.; Mattison, N. T.; O'Carroll, D. M.; Whelton, A. J.; Uddin, N.; Nguyen, T.; Huang, Q.; Henry, T. B.; Holbrook, R. D.; et al. Potential release pathways, environmental fate, and ecological risks of carbon nanotubes. *Environ. Sci. Technol.* **2011**, *45*, 9837−9856.

(6) Allen, B. L.; Kichambare, P. D.; Gou, P.; Vlasova, I. I.; Kapralov, A. A.; Konduru, N.; Kagan, V. E.; Star, A. Biodegradation of single-walled carbon nanotubes through enzymatic catalysis. *Nano Lett.* **2008**, *8*, 3899−3903.

(7) Allen, B. L.; Kotchey, G. P.; Chen, Y.; Yanamala, N. V. K.; Klein-Seetharaman, J.; Kagan, V. E.; Star, A. Mechanistic investigations of horseradish peroxidase-catalyzed degradation of single-walled carbon nanotubes. *J. Am. Chem. Soc.* **2009**, *131*, 17194−17205.

(8) Hersam, M. C. Progress towards monodisperse single-walled carbon nanotubes. *Nat. Nanotechnol.* **2008**, *3*, 387−394.

(9) Moore, V. C.; Strano, M. S.; Haroz, E. H.; Hauge, R. H.; Smalley, R. E.; Schmidt, J.; Talmon, Y. Individually suspended single-walled carbon nanotubes in various surfactants. *Nano Lett.* **2003**, *3*, 1379−1382.

(10) Gandra, N.; Chiu, P. L.; Li, W.; Anderson, Y. R.; Mitra, S.; He, H.; Gao, R. Photosensitized singlet oxygen production upon two-photon excitation of single-walled carbon nanotubes and their functionalized analogues. *J. Phys. Chem. C* **2009**, *113*, 5182−5185.

(11) Chen, C.-Y.; Jafvert, C. T. Photoreactivity of carboxylated single-walled carbon nanotubes in sunlight: Reactive oxygen species production in water. *Environ. Sci. Technol.* **2010**, *44*, 6674−6679.

(12) Chen, C.-Y.; Jafvert, C. T. The role of surface functionalization in the solar light-induced production of reactive oxygen species by single-walled carbon nanotubes in water. *Carbon* **2011**, *49*, 5099−5106.

(13) Chae, S.-R.; Watanabe, Y.; Wiesner, M. R. Comparative photochemical reactivity of spherical and tubular fullerene nanoparticles in water under ultraviolet (UV) irradiation. *Water Res.* **2011**, *45*, 308−314.

(14) Petersen, E. J.; Tu, X.; Dizdaroglu, M.; Zheng, M.; Nelson, B. C. Protective roles of single-wall carbon nanotubes in ultrasonication-induced DNA base damage. *Small* **2013**, *9*, 205−208.

(15) Alvarez, N. T.; Kittrell, C.; Schmidt, H. K.; Hauge, R. H.; Engel, P. S.; Tour, J. M. Selective photochemical functionalization of surfactant-dispersed single wall carbon nanotubes in water. *J. Am. Chem. Soc.* **2008**, *130*, 14227−14233.

(16) Zhang, M.; Yudasaka, M.; Miyauchi, Y.; Maruyama, S.; Iijima, S. Changes in the fluorescence spectrum of individual single-wall carbon nanotubes induced by light-assisted oxidation with hydroperoxide. *J. Phys. Chem. B* **2006**, *110*, 8935−8940.

(17) Yudasaka, M.; Zhang, M.; Iijima, S. Diameter-selective removal of single-wall carbon nanotubes through light-assisted oxidation. *Chem. Phys. Lett.* **2003**, *374*, 132−136.

(18) Hyung, H.; Fortner, J. D.; Hughes, J. B.; Kim, J.-H. Natural organic matter stabilizes carbon nanotubes in the aqueous phase. *Environ. Sci. Technol.* **2007**, *41*, 179−184.

(19) Lin, D.; Xing, B. Tannic acid adsorption and its role for stabilizing carbon nanotube suspensions. *Environ. Sci. Technol.* **2008**, *42*, 5917−5923.

(20) Bouchard, D.; Zhang, W.; Powell, T.; Rattanaudompol, U. Aggregation kinetics and transport of single-walled carbon nanotubes at low surfactant concentrations. *Environ. Sci. Technol.* **2012**, *46*, 4458−4465.

(21) Chowdhury, I.; Duch, M. C.; Gits, C. C.; Hersam, M. C.; Walker, S. L. impact of synthesis methods on the transport of single walled carbon nanotubes in the aquatic environment. *Environ. Sci. Technol.* **2012**, *46*, 11752−11760.

(22) Han, Z.; Zhang, F.; Lin, D.; Xing, B. Clay minerals affect the stability of surfactant-facilitated carbon nanotube suspensions. *Environ. Sci. Technol.* **2008**, *42*, 6869−6875.

(23) Page, S. E.; Arnold, W. A.; McNeill, K. Assessing the contribution of free hydroxyl radical in organic matter-sensitized photohydroxylation reactions. *Environ. Sci. Technol.* **2011**, *45*, 2818−2825.

(24) Latch, D. E.; McNeill, K. Microheterogeneity of singlet oxygen distributions in irradiated humic acid solutions. *Science* **2006**, *311*, 1743−1747.

(25) Zepp, R. G.; Hoigne, J.; Bader, H. Nitrate-induced photo-oxidation of trace organic chemicals in water. *Environ. Sci. Technol.* **2011**, *21*, 443−450.

(26) Zepp, R. G.; Faust, B. C.; Hoigne, J. Hydroxyl radical formation in aqueous reactions (pH 3−8) of iron(II) with hydrogen peroxide: The photo-Fenton reaction. *Environ. Sci. Technol.* **1992**, *26*, 313−319.

(27) Kitiyanan, B.; Alvarez, W. E.; Harwell, J. H.; Resasco, D. E. Controlled production of single-wall carbon nanotubes by catalytic decomposition of CO on bimetallic Co−Mo catalysts. *Chem. Phys. Lett.* **2000**, *317*, 497−503.

(28) Bronikowski, M. J.; Willis, P. A.; Colbert, D. T.; Smith, K. A.; Smalley, R. E. Gas-phase production of carbon single-walled nanotubes

from carbon monoxide via the HiPco process: A parametric study. *J. Vac. Sci. Technol., A* **2001**, *19*, 1800−1805.
(29) O'Connell, M. J.; Bachilo, S. M.; Huffman, C. B.; Moore, V. C.; Strano, M. S.; Haroz, E. H.; Rialon, K. L.; Boul, P. J.; Noon, W. H.; Kittrell, C.; et al. Band gap fluorescence from individual single-walled carbon nanotubes. *Science* **2002**, *297*, 593−596.
(30) Strano, M. S.; Doorn, S. K.; Haroz, E. H.; Kittrell, C.; Hauge, R. H.; Smalley, R. E. Assignment of (n, m) Raman and optical features of metallic single-walled carbon nanotubes. *Nano Lett.* **2003**, *3*, 1091−1096.
(31) Haggenmueller, R.; Rahatekar, S. S.; Fagan, J. A.; Chun, J.; Becker, M. L.; Naik, R. R.; Krauss, T.; Carlson, L.; Kadla, J. F.; Trulove, P. C.; et al. Comparison of the quality of aqueous dispersions of single wall carbon nanotubes using surfactants and biomolecules. *Langmuir* **2008**, *24*, 5070−5078.
(32) Hou, W.-C.; Stuart, B.; Howes, R.; Zepp, R. G. Sunlight-driven reduction of silver ions by natural organic matter: Formation and transformation of silver nanoparticles. *Environ. Sci. Technol.* **2013**, *47*, 7713−7721.
(33) Strano, M. S.; Huffman, C. B.; Moore, V. C.; O'Connell, M. J.; Haroz, E. H.; Hubbard, J.; Miller, M.; Rialon, K.; Kittrell, C.; Ramesh, S.; et al. Reversible, band-gap-selective protonation of single-walled carbon nanotubes in solution. *J. Phys. Chem. B* **2003**, *107*, 6979−6985.
(34) Reich, S.; Thomsen, C.; Ordejón, P. Electronic band structure of isolated and bundled carbon nanotubes. *Phys. Rev. B: Condens. Matter Mater. Phys.* **2002**, *65*, No. 155411.
(35) Bahr, J. L.; Tour, J. M. Covalent chemistry of single-wall carbon nanotubes. *J. Mater. Chem.* **2002**, *12*, 1952−1958.
(36) Rocha, J.-D. R.; Bachilo, S. M.; Ghosh, S.; Arepalli, S.; Weisman, R. B. Efficient spectrofluorimetric analysis of single-walled carbon nanotube samples. *Anal. Chem.* **2011**, *83*, 7431−7437.
(37) Schierz, A.; Parks, A. N.; Washburn, K. M.; Chandler, G. T.; Ferguson, P. L. Characterization and quantitative analysis of single-walled carbon nanotubes in the aquatic environment using near-infrared fluorescence spectroscopy. *Environ. Sci. Technol.* **2012**, *46*, 12262−12271.
(38) Von der Kammer, F.; Ferguson, P. L.; Holden, P. A.; Masion, A.; Rogers, K. R.; Klaine, S. J.; Koelmans, A. A.; Horne, N.; Unrine, J. M. Analysis of engineered nanomaterials in complex matrices (environment and biota): General considerations and conceptual case studies. *Environ. Toxicol. Chem.* **2012**, *31*, 32−49.
(39) Strano, M. S.; Dyke, C. A.; Usrey, M. L.; Barone, P. W.; Allen, M. J.; Shan, H.; Kittrell, C.; Hauge, R. H.; Tour, J. M.; Smalley, R. E. Electronic structure control of single-walled carbon nanotube functionalization. *Science* **2003**, *301*, 1519−1522.
(40) O'Connell, M. J.; Eibergen, E. E.; Doorn, S. K. Chiral selectivity in the charge-transfer bleaching of single-walled carbon-nanotube spectra. *Nat. Mater.* **2005**, *4*, 412.
(41) McDonald, T. J.; Blackburn, J. L.; Metzger, W. K.; Rumbles, G.; Heben, M. J. Chiral-selective protection of single-walled carbon nanotube photoluminescence by surfactant selection. *J. Phys. Chem. C* **2007**, *111*, 17894−17900.
(42) Piao, Y.; Meany, B.; Powell, L. R.; Valley, N.; Kwon, H.; Schatz, G. C.; Wang, Y. Brightening of carbon nanotube photoluminescence through the incorporation of sp3 defects. *Nat. Chem.* **2013**, *5*, 840−845.
(43) Xu, G.; Chance, M. R. Hydroxyl radical-mediated modification of proteins as probes for structural proteomics. *Chem. Rev.* **2007**, *107*, 3514−3543.
(44) Lundeen, R. A.; McNeill, K. Reactivity differences of combined and free amino acids: Quantifying the relationship between three-dimensional protein structure and singlet oxygen reaction rates. *Environ. Sci. Technol.* **2013**, *47*, 14215−14223.
(45) Lin, S.; Blankschtein, D. Role of the bile salt surfactant sodium cholate in enhancing the aqueous dispersion stability of single-walled carbon nanotubes: a molecular dynamics simulation study. *J. Phys. Chem. B* **2010**, *114*, 15616−15625.
(46) Usrey, M. L.; Lippmann, E. S.; Strano, M. S. Evidence for a two-step mechanism in electronically selective single-walled carbon nanotube reactions. *J. Am. Chem. Soc.* **2005**, *127*, 16129−16135.
(47) Tummala, N. R.; Striolo, A. SDS surfactants on carbon nanotubes: Aggregate morphology. *ACS Nano* **2009**, *3*, 595−602.
(48) Xu, Z.; Yang, X.; Yang, Z. A molecular simulation probing of structure and interaction for supramolecular sodium dodecyl sulfate/single-wall carbon nanotube assemblies. *Nano Lett.* **2010**, *10*, 985−991.
(49) Hilmer, A. J.; McNicholas, T. P.; Lin, S.; Zhang, J.; Wang, Q. H.; Mendenhall, J. D.; Song, C.; Heller, D. A.; Barone, P. W.; Blankschtein, D.; et al. Role of adsorbed surfactant in the reaction of aryl diazonium salts with single-walled carbon nanotubes. *Langmuir* **2012**, *28*, 1309−1321.